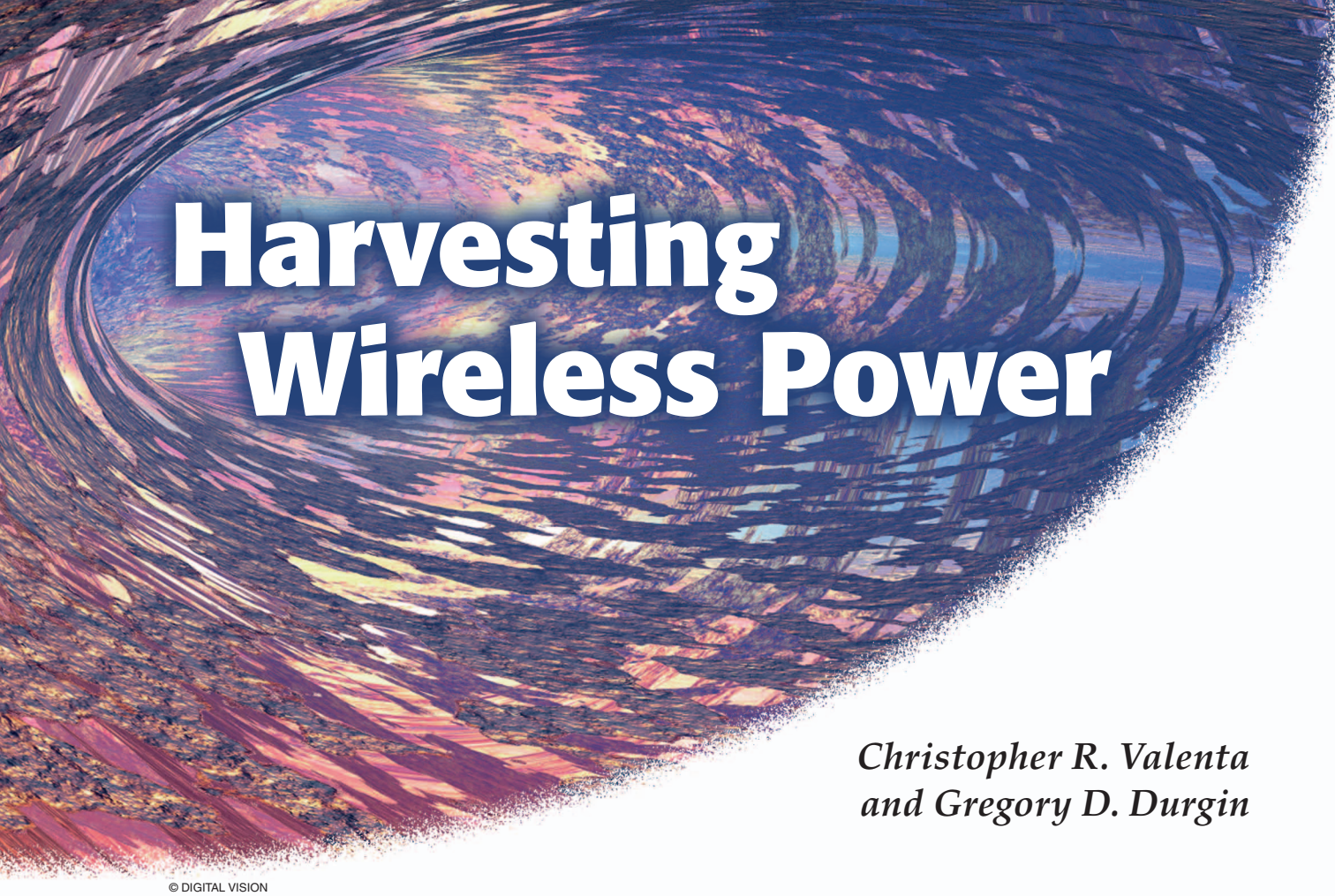

Harvesting Wireless Power

Christopher R. Valenta and Gregory D. Durgin

The idea of wireless power transfer (WPT) has been around since the inception of electricity. In the late 19th century, Nikola Tesla described the freedom to transfer energy between two points without the need for a physical connection to a power source as an "all-surpassing importance to man" [1]. A truly wireless device, capable of being remotely powered, not only allows the obvious freedom of movement but also enables devices to be more compact by removing the necessity of a large battery. Applications could leverage this reduction in size and weight to increase the feasibility of concepts such as paper-thin, flexible displays [2], contact-lens-based augmented reality [3], and smart dust [4], among traditional point-to-point power transfer applications. While several methods of wireless power have been introduced since Tesla's work, including near-field magnetic resonance and inductive coupling, laser-based optical power transmission, and far-field RF/microwave energy transmission, only RF/microwave and laser-based systems are truly long-range methods. While optical power transmission certainly has merit, its mechanisms are outside of the scope of this article and will not be discussed.

Two major communities have made significant contributions toward fulfilling Tesla's dream of wireless power: space-based solar power (SSP) or solar powered satellite (SPS) and RF identification (RFID). Though still in the experimental stage, researchers working in SPS have made advancements in energy conversion at great distances and high powers (greater than 1 W) to enable electricity to be shared via radio waves, namely collecting solar energy in orbital stations around earth and beaming it to ground stations via microwave power transfer [5], [6], [7]. Meanwhile the RFID community has focused on the ultra-low power harvesting (usually much less than 1 W) necessary to provide energy for wireless, batteryless RFID tags and backscatter sensors [8]. Future development in WPT will certainly leverage the work of both SPS

Christopher R. Valenta (christopher.valenta@gatech.edu) is with the Electro-optical Systems Laboratory, Georgia Tech Research Institute, Atlanta, and Gregory D. Durgin (durgin@ece.gatech.edu) is with the Department of Electrical and Computer Engineering, Georgia Institute of Technology, Atlanta.

Digital Object Identifier 10.1109/MMM.2014.2309499
Date of publication: 7 May 2014

and RFID researchers and lead to the deployment of efficient, far-field, wireless power systems.

A survey of current trends in WPT including state-of-the-art energy harvester efficiencies shows that much progress has been made since the early days of SPS and RFID. Research has documented that the efficiency of diode-based energy harvesters is nonlinear and greatly depends on the input power level. Generally speaking, efficiency improves as input power rises, but there are diminishing returns and limitations on the maximum possible energy harvesting efficiency. As research progresses, applications within SPS, RFID, and future unknown areas will benefit from the highest realizations of Tesla's original concept.

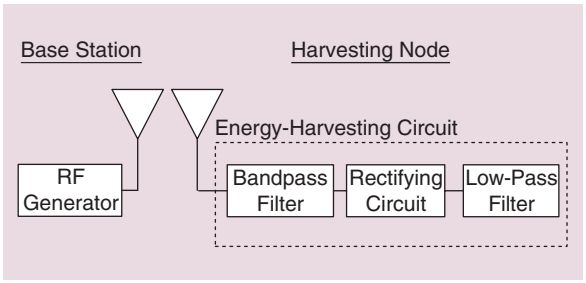

Figure 1. *A WPT system consists of an RF/microwave generator and transmit antenna(s) on the base station side. The RF-to-dc conversion piece of the system consists of one or many receive antennas, matching networks, rectifying circuits, and low-pass filters.*

Wireless Power Transfer Systems

RF/microwave WPT systems have several core components that allow energy to flow between two points in space. These core components are illustrated in Figure 1. First, RF/microwave power must be generated at the base station typically via a magnetron or solid-state source. This choice is usually dominated by efficiency, cost, and desired transmit power [6]. The antenna directionality and polarization is usually dictated by the application, but total transmitted power must obey regulatory and safety standards [9].

After the base station-radiated energy propagates through the channel between the two locations, the harvesting node must capture it. The harvesting node has an energy conversion circuit consisting of a receive antenna(s), combination matching network/bandpass filter, rectifying circuit, and low-pass filter. The bandpass filter helps to ensure that the antenna is correctly matched to the rectifying circuit and that harmonics generated by the rectifying element are not reradiated to the environment. The rectifying circuit can exist in a variety of topologies that will be discussed later but usually involves some number of diodes and capacitors. Finally, an output low-pass filter removes the fundamental and harmonic frequencies from the output, sets the output impedance, and stores charge for consumption.

RF Energy-Harvesting Principles

Nearly all modern energy-harvesting circuits use semiconductor-based rectifying elements in a variety of topologies to convert RF to dc power. (Early methods of RF to dc conversion used microwave heating principles along with closed-spaced, thermionic diodes [10].) While semiconductors are individually able to handle relatively small amounts of power (for WPT applications), their low cost and small form factor makes them ideal for a variety of applications. In SPS systems, Schottky diodes are chosen because of their low voltage threshold and lower junction capacitance than PN diodes [11]. This low threshold allows for more efficient operation at low powers, and the low junction capacitance increases the maximum frequency at which the diode can operate. To produce large amounts of power for SPS systems, large arrays of RF rectifiers are used. Standard CMOS processes do not support Schottky diode fabrication, so discrete components are typically used in SPS harvesting arrays.

On the other hand, RFID applications leverage CMOS technology with diode-connected transistors that significantly increases the energy-harvester efficiency at lower powers because of lower parasitic values and customizable rectifiers. Furthermore, digital logic can be incorporated onto the same die. The ultra-low power levels needed by these realized electronics along with the cost savings by incorporating the entire device on a single integrated circuit (IC) (low cost is essential for the RFID market) make CMOS processes the dominating technology for RFID energy harvesters.

Diode Rectifier Behavior

Diodes are typically modeled according to the nonlinear relationship shown in Figure 2. This I-V curve is characterized by three major regions. For low voltages below the reverse breakdown voltage V_{br}, the diode is said to be reverse biased and will conduct in the reverse direction. Between V_{br} and V_T, the turn-on voltage, the diode is off and only a very small amount of leakage current will flow. Above V_T, the diode is said to be forward biased and current will flow proportionally to voltage.

When a diode is used as a rectifier, the maximum dc voltage across the diode $V_{o,dc}$ is limited by the reverse breakdown voltage as shown by

$$V_{o,\mathrm{DC}} = \frac{V_{br}}{2}. \tag{1}$$

This limitation occurs because this dc voltage will limit the maximum peak-to-peak ac voltage of the input waveform. Since the input waveform is symmetrical in the case of continuous wave excitation, the maximum peak-to-peak voltage is equal to the breakdown voltage V_{br}, and the maximum dc voltage is (1). If the peak-to-peak voltage is larger than this value, the waveform will exceed the breakdown voltage and

While related to energy-harvester efficiency, sensitivity is defined as the minimum power necessary to power an integrated circuit.

the dc level will no longer increase. Consequently, the maximum dc power P_{DCmax} is limited by

$$P_{\mathrm{DCmax}} = \frac{V_{br}^2}{4R_L}. \tag{2}$$

The load resistance R_L, which guarantees the maximum efficiency for applications operating near the breakdown voltage is typically 1.3 to 1.4 times the diode intrinsic/video resistance [12]. This value corresponds as a tradeoff between equal resistances for maximum power transfer and a large load resistance to minimize the losses associated with the diode turn-on voltage.

Energy-Harvesting Circuit Characterization

Literature characterizes energy-harvesting circuits by two different metrics—efficiency and sensitivity. Efficiency can be expressed as a total energy-harvesting circuit efficiency or a power-conversion efficiency. In both cases, the desired power P_{outDC} is the dc voltage V_{outDC} across a load resistance R_L defined in (3)

$$P_{\mathrm{outDC}} = \frac{V_{\mathrm{outDC}}^2}{R_L}. \tag{3}$$

This output power represents the useful power that can be provided to the device circuitry. If the received power at the input to the energy-harvesting circuit is defined as P_{inEH}, then the charge-pump efficiency η_{EH} is

$$\eta_{EH} = \frac{P_{\mathrm{outDC}}}{P_{\mathrm{inEH}}} = \frac{\frac{V_{\mathrm{outDC}}^2}{R_L}}{P_{\mathrm{inEH}}}. \tag{4}$$

The inherent nonlinearity of diodes means that energy-harvesting circuits will also reflect some power when not completely matched. In literature, a power-conversion efficiency η_{PC} is also given as

$$\eta_{\mathrm{PC}} = \frac{P_{\mathrm{outDC}}}{P_{\mathrm{inCP}}} = \frac{\frac{V_{\mathrm{outDC}}^2}{R_L}}{P_{\mathrm{inEH}} - P_{\mathrm{reflected}}}, \tag{5}$$

where P_{inCP} is the power delivered into the charge pump neglecting reflected power $P_{\mathrm{reflected}}$ due to impedance mismatch. Power-conversion efficiency decouples the issues in matching the energy-harvesting circuit and rather focuses on its intrinsic ability to convert RF power to dc. Note that the largest η_{EH} can ever be is η_{PC}. This instance would only occur if the antenna is perfectly matched to the energy-harvesting circuit at the input power level [12]. Consequently, the input power to the antenna P_{inEH} is equal to the power delivered into the energy-harvesting circuit P_{inCP}. The SPS community typically cites charge-pump efficiency as its principle figure of merit since the end-to-end delivered power is of paramount importance for these types of systems.

While related to energy-harvester efficiency, sensitivity is defined as the minimum power necessary to power an IC. Inherently, this definition depends on the IC technology and application as different sensors and protocols can cause the sensitivity number to be larger. As many RFID researchers operate in this semiconductor regime, they often cite sensitivity as their evaluation metric. This article will use the former metric of charge-pump efficiency to compare energy-harvesting circuits as it can be used to universally compare the effectiveness of energy conversion.

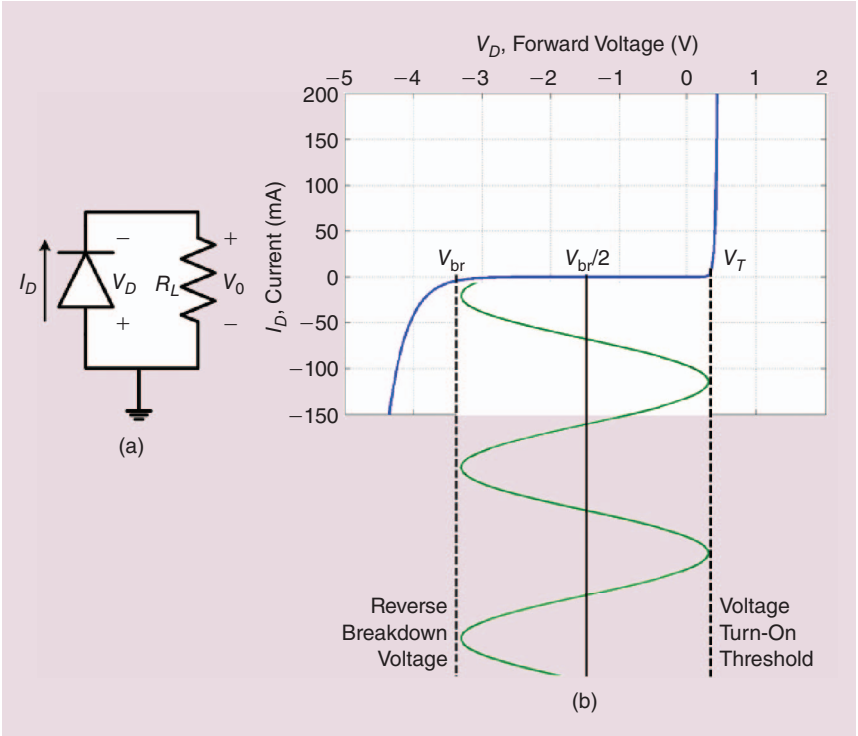

Figure 2. *A typical diode I-V curve with annotated breakdown and turn-on voltages. The schematic in (a) assumes that all reactive elements have been tuned out, and a sufficient RF power exists across the diode to generate a dc voltage across the output resistor R_L.*

Energy-Harvesting Circuit Losses

While highly efficient energy harvesters are desirable, a variety of loss mechanisms make it difficult to achieve high efficiencies, especially in nonlinear devices such as the diodes and diode-connected transistors. Figure 3 illustrates the relationship between some of these losses and the energy-harvesting efficiency.

- **Threshold and reverse-breakdown voltage:** Typically the most important parameter for diode efficiency is the threshold or turn-on voltage V_T. This parameter limits efficiency at low powers as noted by "V_T Effect" in Figure 3. Unless sufficient power is incident on the energy harvester, there is not enough energy to overcome this barrier and charge the output capacitor. Diode reverse breakdown voltage V_{br} also limits diode efficiency as this will allow energy to short the diode demonstrated by the curve "V_{br} Effect." This situation will occur at larger power levels when the diode dc bias is equal to half the breakdown voltage as previously discussed. Note that while the efficiency curve decreases above this point, dc output power will remain constant.
- **Impedance matching:** When an energy-harvesting circuit is not properly matched to its antenna, part of the incident power from the antenna will be reflected back to the environment and not absorbed. If the power is not absorbed, then the available power for rectification is automatically reduced. Matching is especially difficult in energy-harvesting circuit design as the impedance will change as a function of both frequency and input power due to the nonlinearity of the rectifying elements shown by the diode model in Figure 4 and illustrated in Figure 5.
- **Device parasitics:** Device parasitics can also cause a significant decrease in efficiency. Diode junction resistance R_s can limit diode efficiencies as current flowing through the diode will dissipate power in the semiconductor junction [13]. At high frequencies, junction capacitance C_j and package inductances also lead to significant performance degradations because of cutoff issues. Typically, the junction capacitance limits the maximum frequency at which the diode can operate. Additional package parasitics exist but are not discussed here as there are numerous sources that list these. Furthermore, traditional losses in the substrate and transmission lines may also play a significant role in energy harvester efficiency depending on the substrate and line lengths chosen.
- **Harmonic generation:** While providing a means to convey RF energy to dc, the diode nonlinearity is also a source of loss. When operating, the diode will produce frequency harmonics from the incident power, which reduces the proportion of energy that gets converted to dc resulting in a lower energy harvester efficiency. As the incident voltage continues to increase, the energy lost to harmonics further increases. An optimal efficiency level corresponds to tradeoffs between harmonic generation, reverse breakdown effects, and threshold voltage.

Diode Parameter Behavior

Figure 6 shows the energy-harvesting efficiency of a single, commercially available, Avago HSMS-286x silicon-nickel Schottky diode as a function of power at 5.8 GHz delivered from a 50-Ω source. Each subplot shows the variation in performance as a single parameter

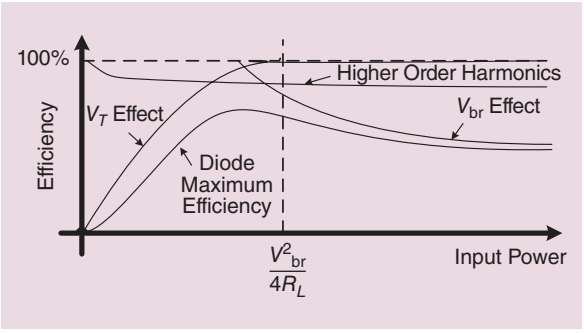

Figure 3. *The general relationship between the efficiency and losses in microwave energy conversion circuits as a function of input power (recreated from [13]). At low powers, the efficiency is limited by the input signal ability to surpass the diode turn-on threshold voltage (labeled "V_T Effect"). As the power continues to increase, the efficiency will increase along with harmonics. At higher powers, the diode reverse breakdown voltage limits the efficiency (labeled "V_{br} Effect"). A maximum conversion efficiency occurs between these points.*

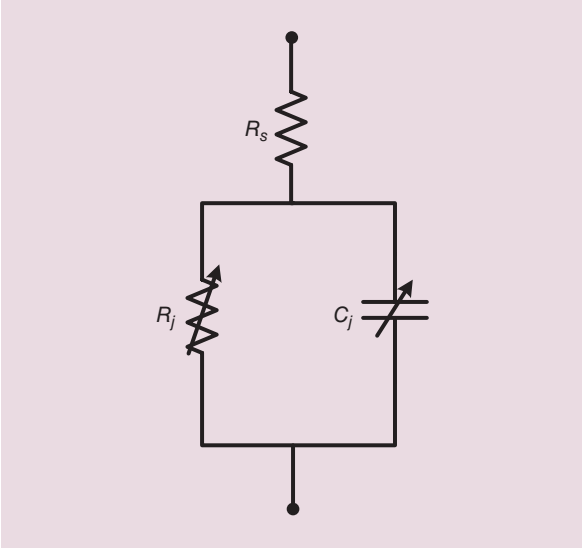

Figure 4. *A standard Schottky diode model. A resistance R_s is in series with a variable junction resistance R_j in parallel with a variable junction capacitance C_j that change as a function of input power. The nonlinearity of Schottky diodes in energy harvesting circuits makes impedance matching a challenging endeavor.*

changes, and all other parameters are held constant according to the values in the table sand using a load resistance $R_L = 327\ \Omega$. It should be noted that these changes cannot occur alone. Adjusting one parameter will inevitably cause changes in others due to the underlying semiconductor relationships. For the point of illustration, these effects are not included.

These curves are generated using the theory discussed by Yoo and Chang in [13] for the efficiency of a diode with resistive load under a single frequency excitation. This derivation assumes no package parasitic elements and no harmonic generation. The loss factors that are considered are the diode threshold voltage V_T, junction capacitance C_j, and the diode series resistance R_s. Thus, actual conversion efficiencies will be lower because of harmonic generation, parasitic elements, and impedance mismatch.

Figure 6 shows several interesting trends. Figure 6(a) demonstrates that a low turn-on threshold is required for efficient, low-power operation. As the turn-on threshold voltage is decreased, the energy conversion efficiency at a given power increases. This phenomenon occurs because the same power level can more easily overcome the turn-on voltage limitation. In traditional

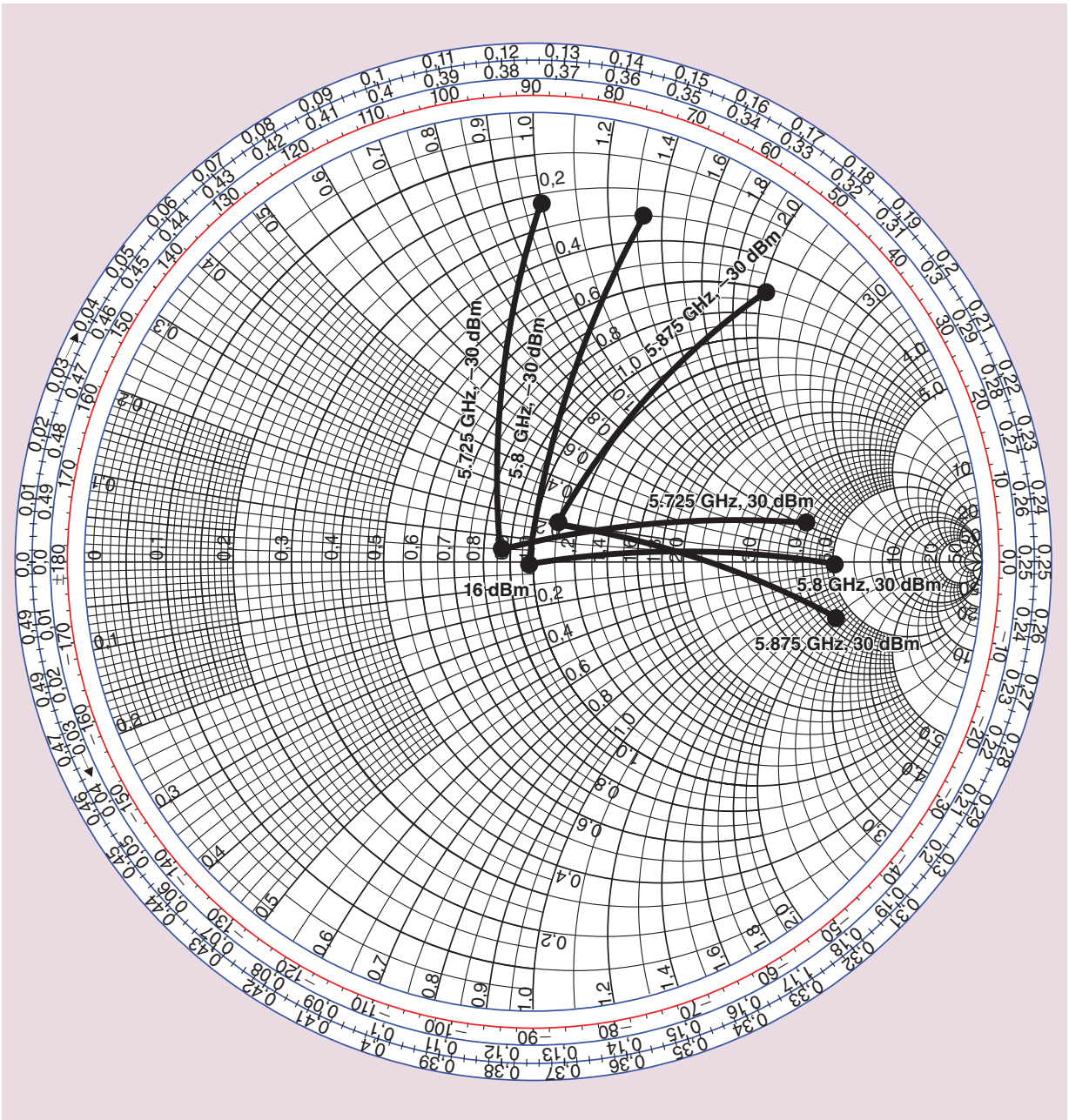

Figure 5. *Impedance of a single-shunt rectenna with a 316-Ω load matched at 5.8 GHz and 16-dBm input power. The large range of possible impedances makes it difficult for an energy-harvesting circuit to work efficiently over a wide range of input powers and frequencies because of the reflected power due to impedance mismatch [14].*

semiconductor processes, lowering the threshold voltage usually lowers the breakdown voltage [15].

Figure 6(b) shows that a large reverse breakdown voltage allows a larger allowable input/output voltage/power as noted by (1). As the reverse breakdown voltage increases, the maximum allowable output power level increases; conversion efficiency of the low powers remains unchanged. Figure 6(c) shows that the junction capacitance limits the maximum frequency for which a diode can operate. As is shown, 2.4 GHz and 5.8 GHz have approximately the same energy conversion efficiency because the 0.18 pF junction capacitance along with the 6Ω series resistance does not filter out much power at these frequencies. However, when the frequency is increased to 10 GHz and 35 GHz, the conversion efficiency begins to decrease.

Figure 6(d) demonstrates that when the series resistance increases, the energy conversion efficiency decreases. This result is due to normal resistance losses in the semiconductor junction. Finally, Figure 6(e) demonstrates the energy conversion efficiency dependence on the load resistance. As this resistance increases, the efficiency increases, but the maximum input power level decreases. This decrease in maximum power is due to the larger resistance producing the same voltage for a smaller current, which limits the maximum input power

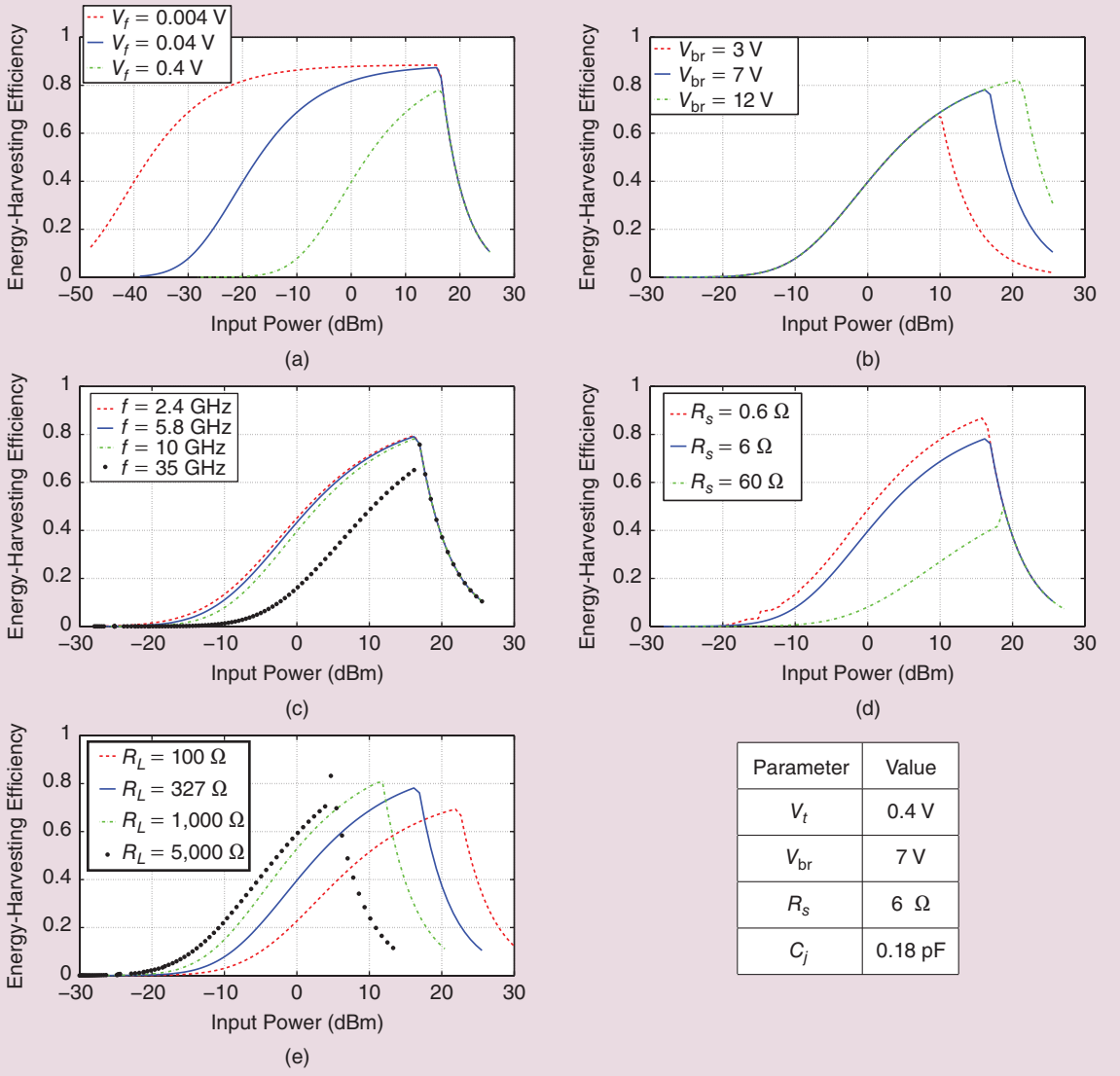

Parameter	Value
V_t	0.4 V
V_{br}	7 V
R_s	6 Ω
C_j	0.18 pF

Figure 6. *The theoretical energy-harvesting efficiency of a single, silicon-nickel Schottky diode under CW excitation delivered from a 50-Ω source. This figure illustrates (a) the performance variation when various diode parameters (voltage threshold V_T in, (b) breakdown voltage V_{br} in, (c) input frequency in, (d) series resistance R_s, and (e) load resistance R_L are varied. Parameters are varied about those of a standard Avago HSMS-286x diode as shown in the enclosed table. (a) Variation of threshold voltage V_t, (b) variation of breakdown voltage V_{br}, (c) variation of input frequency, (d) variation of series resistance R_S, and (e) variation of load resistance R_L.*

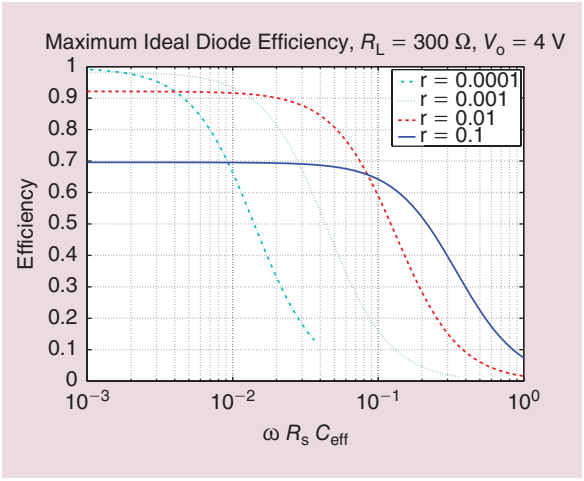

Figure 7. *The maximum efficiency of an ideal diode ($V_t = 0$ V and $V_{br} = \infty$) for various values of r ($r = R_S/R_L$). A low-pass filter effect is due to the diode junction capacitance and series resistance. Maximum efficiency occurs in the passband of this filter and increases with decreasing values of the series resistance.*

as shown by (2). The increase in efficiency is caused by the reduction of the loss of power in R_s and the loss of power in the diode.

Maximum Energy Conversion Efficiency

As previously stated, the maximum energy conversion efficiency of an energy-harvesting circuit is limited by impedance matching, device parasitics, and harmonic generation. Using the same method from [13], the efficiency of an ideal diode is plotted in Figure 7 as a function of frequency ω, diode junction series resistance R_s, and effective junction capacitance C_{eff} (see [13] for a description of this parameter). Various values of r are also plotted ($r = R_s/R_L$). In this case, an ideal diode is defined as one that has an infinite breakdown voltage and zero turn-on voltage. All other assumptions from this derivation hold as well. Actual diode performance will typically be less as additional loss mechanisms will be encountered and breakdown and turn-on voltages will cause additional losses.

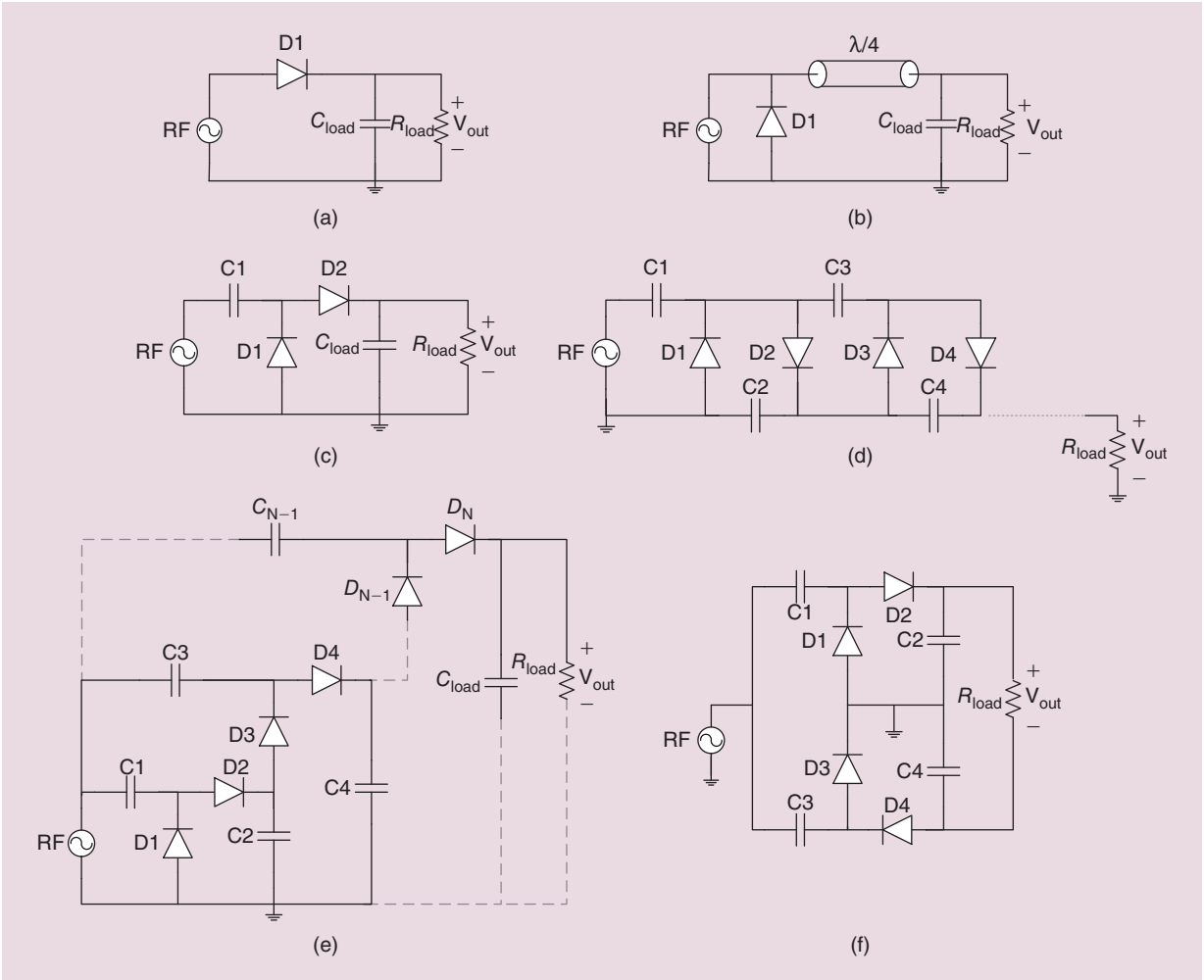

Figure 8. *Various energy-harvesting circuit topologies used in RFID and SPS applications. (a) Half-wave rectifier, (b) single shunt rectenna, (c) single stage voltage multiplier, (d) Cockcroft-Walton/Greinacher/Villard charge pump, (e) Dickson charge pump, and (f) modified Cockcroft-Walton/Greinacher charge pump.*

Two main points can be seen in Figure 7. First, a frequency selective behavior is exhibited by the efficiency. This behavior is due to the diode junction resistance R_j functioning in parallel with the diode junction capacitance C_j shown in the diode equivalent circuit in Figure 4. Thus as ω and/or C_{eff} are increased, efficiency decreases because of the low-pass filter response of this circuit. Likewise, efficiency decreases as R_s increases due to traditional resistive losses. Second, it can be seen that for small values of r, which corresponds to small values of R_s or large values of R_L, the maximum efficiency is larger. This larger efficiency is a result of a lower loss due to this junction series resistance. However, this lower resistance also means that for a fixed junction capacitance, the diode is most efficient at low frequencies. Therefore, there will be a tradeoff in diode performance at high frequencies assuming a constant junction capacitance. Highly efficient diodes are possible, but this performance will occur at low frequencies. High frequency operation will require a larger junction series resistance and/or smaller junction capacitance.

The ideal energy harvester has to accommodate a low sensitivity, high efficiency, wide power range, and a necessarily high-frequency response. The tradeoff between threshold voltage and reverse breakdown voltage in a diode imposes a tradeoff in the energy harvester sensitivity and the range of input powers that the node may operate. Meanwhile, a larger series resistance in the diode provides the high frequency response but limits efficiency as seen in Figure 6.

Energy-Harvesting Circuit Topologies

The main purpose of an energy-harvesting circuit is to convert received RF energy into dc. While there are multiple methods of doing this, diode-based rectifier circuits are most commonly used. Figure 8 illustrates some of the most common topologies. The SPS community typically utilizes rectenna-based designs as high efficiency is paramount, and large power densities are available. Schottky diodes have larger power handling abilities than their CMOS counterparts, and large output voltage are unnecessary.

In contrast, battery-free sensor designers and the RFID community use charge pump topologies for energy harvesting. While rectennas can efficiently harvest RF energy, the dc voltages produced are not sufficient to drive the logic level of modern electronics (1–3 V) at the low levels encountered in RFID applications. Charge pumps not only rectify RF to dc but also step up the voltage to usable levels by means of cascaded diode-capacitor stages. Each stage uses the previous stage for biasing reference, and as a result, a larger voltage can be obtained. Furthermore, the RFID community can leverage CMOS processes to create low-loss harvesters and manipulate diode properties. Note that a combination of these approaches is sometimes used; a rectenna harvests energy to create a low voltage that powers a highly efficient dc-dc converter usually based on the traditional Dickson charge pump [16] to increase the voltage to levels capable of powering the electronics. Note that the original Dickson charge pump utilized low-frequency digital clock signals to increase the dc voltage instead of using an RF signal for this purpose.

State-of-the-Art RF Energy Harvesters

Figure 9 and Tables 1–4 show a survey of the state-of-the-art efficiencies for energy-harvesting devices (note that asterisked efficiencies are those that include antenna

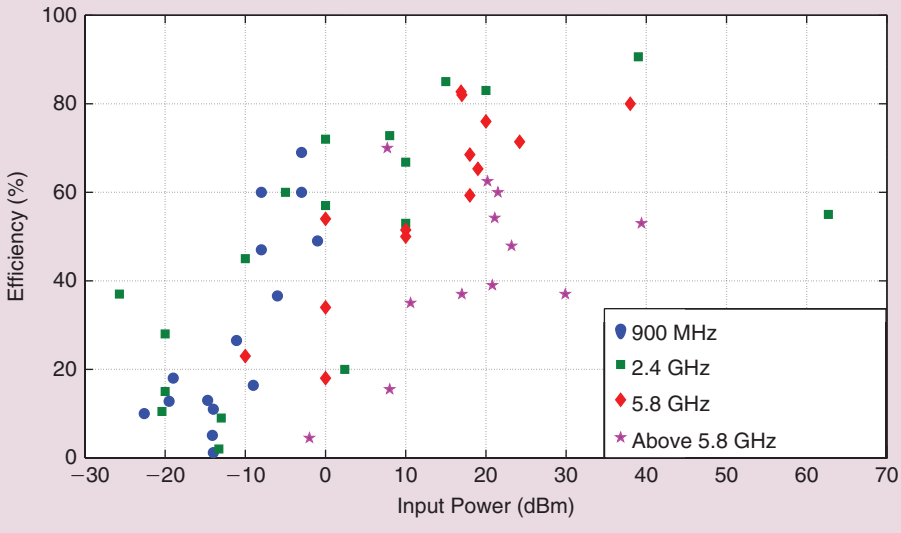

Figure 9. *State-of-the-art RF and microwave-energy conversion efficiencies. A variety of topologies including charge pumps and rectennas are used under a variety of load conditions and technologies (an earlier version of this figure was published in [14]).*

RF/microwave WPT systems have several core components that allow energy to flow between two points in space.

effects in their efficiency calculations. Nonasterisked efficiencies include efficiencies only related to the rectifier). The device efficiencies use a variety of technologies and topologies and use varying loads due to their uses in WPT applications along with wireless, passive nodes such as RFID. These works cover frequencies from 800 MHz up to 94 GHz but principally focus on work in the US ISM bands at 900 MHz, 2.4 GHz, and 5.8 GHz. In some cases, multiband [17]–[20], or wide band [22]–[24] energy harvesters have been utilized to take advantage of ambient RF energy or signals from multiple bands. Additionally, researchers have experimented with designing excitation signals for improved efficiency [25]–[28], [14]. However, this article presents efficiencies for single frequency excitation only. It should be noted that when excitation signals are designed, energy harvester efficiencies can dramatically increase, especially at lower powers.

TABLE 1. State-of-the-art UHF energy conversion efficiencies.

Efficiency (%)	Input Power (dBm)	Frequency (MHz)	Rectifier Element	Source
1.2	−14	950	0.3-μm CMOS transistor	[29]
5.1	−14.1	920	0.18-μm CMOS transistor	[30]
10*	−22.6	906	0.25-μm CMOS transistor	[31]
11	−14	915	90-μm CMOS transistor	[32]
12.8	−19.5	900	0.18-μm CMOS, $CoSi_2$ − Si Schottky	[33]
13	−14.7	900	0.35-μm CMOS transistor	[34]
16.4	−9	963	0.35-μm CMOS transistor	[35]
18	−19	869	0.5-μm CMOS, SiTi Schottky	[36]
26.5	−11.1	900	0.18-μm CMOS transistor	[37]
36.6	−6	963	0.35-μm CMOS transistor	[35]
47	−8	915	0.18-μm CMOS transistor	[38]
49*	−1	900	Skyworks SMS7630 Si Schottky	[17]
60*	−8	906	0.25-μm CMOS transistor	[31]
60	−3	915	0.13-μm CMOS transistor	[39]
69	−3	915	0.18-μm CMOS transistor	[38]

*Asterisked efficiencies are those that include antenna effects in their efficiency calculations. Nonasterisked efficiencies include efficiencies only related to the rectifier.

Several trends are evident in Figure 9. First, as power increases, efficiency tends to increase. This tendency is related to a decrease in the effect of losses due the diode threshold voltage. At high powers, large efficiencies are possible as the energy-harvesting devices are operating in a linear state, far above their diode turn-on voltage. As the power level is reduced, the device efficiency decreases because the diode is "on" for a smaller fraction of the RF wave period. Secondly, as frequency increases, the efficiency of the devices decreases. This observation can be attributed to the higher device parasitic losses encountered at microwave frequencies.

UHF Energy Harvesters

A peculiarity discerned from the graph along with Table 1 is that UHF charge pumps are typically designed for low-power operation below 0 dBm. This design choice is a result of UHF energy harvester research being driven by the RFID community that typically operates in the 865–928 MHz regions. As passive RFID tags must scavenge energy in multipath environments far away from their readers, available energy levels are very low. Consequently, the reported energy levels along with the reported energy harvester efficiencies in the figure correspond to power level cutoffs around approximately –20 dBm. Furthermore, to accommodate sufficiently high-voltage levels to power digital electronics at these very low power levels, UHF energy harvesters have utilized multistage rectifying circuits, such as the Dickson or modified Cockcroft-Walton.

This low operation voltage is possible due to the heavy use of CMOS technology as demonstrated in Table 1. Not only do CMOS processes allow custom-built electronics, which are more efficient and require lower operating voltage than microcontrollers or other external digital devices, but custom rectifying elements are possible. While most standard CMOS processes are incompatible with Schottky diodes due to concerns over cost, some UHF energy harvester

designs have leveraged CMOS-based Schottky diodes [33], [36]. More commonly, diode-connected transistors are used in these topologies. Diode connected transistors can be designed to have a near-zero threshold (zero threshold diodes or transistors are typically those with a forward voltage level of less than 150 mV), which makes them ideal for ultra-low power energy harvesting. While this threshold can be adjusted by appropriately varying typical transistor properties such as the gate length and width and doping level, different topologies have been suggested to further lower the threshold voltage to increase the harvester efficiency at low power levels. Most of these techniques involve some method of providing additional voltage bias that effectively reduces the threshold voltage [40], [31], [32].

Although it is possible to lower a diode-connected transistor threshold voltage by applying a constant dc voltage to a transistor body, the source of this bias is difficult to justify in many energy harvesting applications as this energy source will degrade the overall efficiency. Additionally, the use of non-RF power sources to bias the transistors such as a battery defeats the purpose of traditional passive RFID tags. Other on-chip techniques better lend themselves to the same goal. In [40], Lin et al. used two charge pumps, a primary charge pump and a secondary to bias the primary. However, this technique requires additional chip space, and the limitations of the secondary charge pump are still prevalent. In [31], Le et al. utilized a high-Q resonator along with floating-gate transistors to reduce the threshold voltage. Charge injected into the gate lowers the threshold voltage, but a bias must be held constant to maintain this level. In [32], Papotto et al. utilized a self-compensated transistor threshold voltage methodology relying on transistor body biasing from connected transistor gates to the source of the previous stage.

Microwave Energy Harvesters

Both SPS and RFID applications have numerous advantages in moving to microwave frequencies. Microwave antennas are substantially smaller than some of their UHF and VHF counterparts, and this smaller size helps to reduce the antenna aperture required and to focus the antenna beams more easily. Since the antenna size is the dominating component in the size of a rectenna or RFID-enabled sensor, space can be used more efficiently. This reduction in size (and therefore weight) can help SPS applications reduce the amount of land required for ground-based, power collecting

Nearly all modern energy-harvesting circuits use semiconductor-based rectifying elements in a variety of topologies to convert RF to dc power.

TABLE 2. State-of-the-art RF energy conversion efficiencies in the 2.45-GHz band.

Efficiency (%)	Input Power (dBm)	Frequency (MHz)	Rectifier Element	Source
2.01*	−13.3	2,450	Skyworks SMS7630 Si Schottky	[53]
9*	−13	2,450	Skyworks SMS7630 Si Schottky	[17]
10.5*	−20.4	2,450	Skyworks SMS7630 Si Schottky	[54]
15	−20	2,450	Avago HSMS-2852 Si Schottky	[55]
20*	2.4	3,000	Skyworks SMS7630 Si Schottky (array)	[22]
28	−20	2,450	Avago HSMS-2852 Si Schottky	[56]
37*	−25.7	2,450	Silicon on Saphire 0.5-μm CMOS transistors	[57]
45	−10	2,450	Avago HSMS-2852 Si Schottky	[55]
53	10	2,450	Avago HSMS-2852 Si Schottky	[55]
55*	62.7	2,450	Thermionic	[10]
57	0	2,450	Avago HSMS-282*x* Si Schottky	[58]
60	−5	2,450	Avago HSMS-2852 Si Schottky	[55]
66.8	10	2,450	Avago HSMS-2860 Si Schottky	[18]
72	0	2,100	Avago HSMS-282*x* Si Schottky	[58]
72.8	8	2,450	Skyworks SMS7630 Si Schottky	[52]
83*	20	2,450	M/A-COM 4E1317 GaAs Schottky	[19]
85*	15	2,450	GaAs Schottky	[49]
90.6*	39	2,450	GaAs – Pt Schottky	[12]

*Asterisked efficiencies are those that include antenna effects in their efficiency calculations. Nonasterisked efficiencies include efficiencies only related to the rectifier.

TABLE 3. State-of-the-art microwave-energy conversion efficiencies at 5.8 GHz.

Efficiency (%)	Input Power (dBm)	Frequency (MHz)	Rectifier Element	Source
18*	0	5,800	M/A-COM 4E1317 GaAs Schottky	[19]
23	−10	5,800	Unspecified Schottky	[59]
34*	0	5,800	Avago HSMS-8202 Si Schottky	[60]
50*	10	5,800	M/A-COM 4E1317 GaAs Schottky	[61]
51.5	10	5,800	Avago HSMS-2860 Si Schottky	[18]
54	0	5,800	Unspecified Schottky	[59]
59.3	18	5,800	M/A-COM 4E2054 GaAs Schottky	[62]
65.3	19	5,800	M/A-COM 4E2054 GaAs Schottky	[62]
68.5*	18	5,800	Avago HSMS-8202 Si Schottky	[60]
71.4*	24.2	5,800	HP 5082-2835 GaAs Schottky	[63]
76*	20	5,800	M/A-COM 4E1317 GaAs Schottky	[61]
80*	38	5,870	Si Schottky	[12], [64]
82*	17	5,800	M/A-COM 40150 – 119 Si Schottky	[12]
82.7*	16.9	5,800	M/A-COM 4E1317 GaAs Schottky	[19]

*Asterisked efficiencies are those that include antenna effects in their efficiency calculations. Nonasterisked efficiencies include efficiencies only related to the rectifier.

TABLE 4. State-of-the-art microwave-energy conversion efficiencies above 5.8 GHz.

Efficiency (%)	Input Power (dBm)	Frequency (MHz)	Rectifier Element	Source
62.5	20.2	8,510	M/A-COM 40401 Schottky	[65]
60*	21.5	10,000	Alpha Industries DMK6606 GaAs Schottky	[13]
47.9	23.2	24,000	M/A-COM 4E1317 GaAs Schottky	[66]
54.2	21.1	24,000	M/A-COM MADS-001317-1320AG GaAs Schottky	[67]
4.5*	−2	25,700	M/A-COM 4E2502L Si Schottky	[68]
15.5*	8	25,700	M/A-COM 4E2502L Si Schottky	[68]
35*	10.6	35,000	M/A-COM 4E1317 GaAs Schottky	[69]
37*	17	35,000	Alpha Industries DMK6606 GaAs Schottky	[13]
39*	20.8	35,000	Alpha Industries DMK6606 GaAs Schottky	[13]
53*	39.4	35,000	0.13-μm CMOS Schottky	[20]
70*	7.7	35,000	GaAs Schottky	[70]
37*	29.9	94,000	0.13-μm CMOS Schottky	[20]

*Asterisked efficiencies are those that include antenna effects in their efficiency calculations. Nonasterisked efficiencies include efficiencies only related to the rectifier.

stations, and help RFID applications minimize the profiles of their tags and sensors. The world-wide availability of the unlicensed 5.8-GHz microwave band, an ISM frequency band in the United States, has led research in microwave-power transfer to focus on this frequency. In fact, several other benefits of operating at 5.8 GHz for RFID have been discussed apart from the reduced footprint including the following: greater bandwidth availability, reduced degradations of antenna performance on objects [41], spatial signaling techniques [42]–[44], greater material sensing capability [45], [46], and plasma penetration ability [47], [48] among others.

It is important to note that the majority of UHF charge-pump research has focused on CMOS implementations. This fact is not surprising as an RFID tag cost drops tremendously when the charge pump is integrated with the tag's electronics. However, CMOS processes have yet to mature to an acceptable price point, power handling ability, and efficiency required for microwave energy-harvesting applications. Thus, as discerned from Tables 2, 3, and 4, most of these applications rely on discrete, Schottky diode rectifying elements. It can also be observed from Figure 9 that the majority of microwave work has been done at relatively higher power levels than most of the UHF work. This fact is due to these devices being used for SPS or other predominantly WPT-focused applications. As a result, the multistage topologies used in UHF energy harvester design is unnecessary. Single stage or single diode rectifiers such as the single-shunt rectenna are more common.

Since the majority of these devices rely on discrete Schottky diodes and not custom CMOS transistors, much of the work in these energy harvesters

focuses on choosing the most efficient Schottky diode for the application and on antenna/circuit design and layout optimization. Custom Schottky diodes have been investigated by McSpadden and Chang in [12] and by Brown in [49]. These diodes have performed remarkably well for their applications and have yielded some of the most efficient harvesters to date. More commonly, commercial off-the-shelf components have been used in rectifying elements as their costs are considerably lower. Often times, diodes are used in parallel as an attempt to lower the resistive losses associated with the semiconductor junction. This setup is difficult at higher frequencies because junction capacitances will increase as the diodes are put in parallel.

Other discussed technologies to improve microwave energy harvesting efficiency include highly resonant microwave structures [50] and harmonic terminations [51], [52]. Highly resonant structures help to increase the voltage incident on the rectifying element. However, practical considerations often limit the Q of these resonators. Harmonic terminations such as class-E and class-F rectifiers help to ensure that harmonic frequencies of the excitation frequency are properly terminated and reflected back to the rectifying element to eliminate losses associated with the harmonics.

Conclusion

The WPT community has developed arrays of energy harvesters to enable the theoretical transfer of gigawatts of power from space all the way down to tiny charge pumps capable of extracting usable energy from less than 5 mW of incident power. The choice of rectifying element(s), along with intelligent design and layout of the energy-harvesting circuit, helps to achieve maximum conversion efficiencies an excess of 90%. Utilizing microwave frequencies keeps these devices small and takes advantage of antenna array techniques, although reducing efficiency. Continuing research into WPT technologies along with increasing computational efficiency of electronics will enable numerous new applications in ubiquitous computing and simultaneously benefit SPS applications.

Nikola Tesla described the freedom to transfer energy between two points without the need for a physical connection to a power source as an "all-surpassing importance to man."

References

[1] N. Tesla, "The transmission of electrical energy without wires as a means for furthering peace," *Elect. World Eng.*, pp. 21–24, Jan. 1905.

[2] G. Crawford, *Flexible Flat Panel Displays*. New York: Wiley, 2005.

[3] B. Parviz, "Augmented reality in a contact lens," *IEEE Spectrum*, vol. 46, no. 9, pp. 36–41, Sept. 2009.

[4] B. Warneke, M. Last, B. Liebowitz, and K. Pister, "Smart dust: Communicating with a cubic-millimeter computer," *Computer*, vol. 34, no. 1, pp. 44–51, Jan. 2001.

[5] P. E. Glaser, "Power from the sun: Its future," *Science*, vol. 162, no. 3856, pp. 857–861, Nov. 1968.

[6] N. Shinohara, Wireless power transmission for solar power satellite (SPS). Space Solar Power Institute, Tech. Rep., 2000. [Online]. Available: http://www.sspi.gatech.edu/wptshinohara.pdf

[7] R. M. Dickson, "Power in the sky: Requirements for microwave wireless power beamers for powering high-altitude platforms," *IEEE Microwave Mag.*, vol. 14, pp. 36–47, Apr. 2013.

[8] D. M. Dobkin and S. M. Weigand, "UHF RFID and tag antenna scattering, Part I: Experimental results," *Microwave J., Euro-Global Ed.*, vol. 49, no. 5, pp. 170–190, 2007.

[9] Federal Communications Commission "FCC Rules and Regulations Part 15 Section 247 (15.247)," in "Operation within the bands 902–928 MHz, 2400–2483.5 MHz, and 5725–5850 MHz," Tech. Rep., 2014.

[10] W. Brown, "Experiments in the transportation of energy by microwave beam," *IRE Int. Convention Record*, vol. 12, no. 2, pp. 8–17, 1964.

[11] K. Finkenzeller, *RFID Handbook: Fundamentals and Applications in Contactless Smart Cards and Identification*. New York: Wiley, 2003.

[12] J. McSpadden, L. Fan, and K. Chang, "Design and experiments of a high-conversion-efficiency 5.8-GHz rectenna," *IEEE Trans. Microwave Theory Tech.*, vol. 46, no. 12, p. 8, Dec. 1998.

[13] T. Yoo and K. Chang, "Theoretical and experimental development of 10 and 35 GHz rectennas," *IEEE Trans. Microwave Theory Tech.*, vol. 40, no. 6, p. 8, June 1992.

[14] C. Valenta and G. Durgin, "Rectenna performance under power-optimized waveform excitation," in *Proc. IEEE Int. Conf. RFID*, Apr. 2013, pp. 237–244.

[15] S. Sze, *Semiconductor Devices: Physics and Technology*, 2nd ed. New York: Wiley, 2002.

[16] J. F. Dickson, "On-chip high-voltage generation in MNOS integrated circuits using an improved voltage multiplier technique," *IEEE J. Solid-State Circuits*, vol. SC-11, pp. 374–378, June 1976.

[17] D. Masotti, A. Costanzo, M. Del Prete, and V. Rizzoli, "Genetic-based design of a tetra-band high-efficiency radio-frequency energy harvesting system," *IET Microwaves, Antennas Propagat.*, vol. 7, no. 15, pp. 1254–1263, June 2013.

[18] D. Wang and R. Negra, "Design of a dual-band rectifier for wireless power transmission," in *Proc. 2013 IEEE Wireless Power Transfer*, May 2013, pp. 127–130.

[19] Y. Suh and K. Chang, "A high-efficiency dual-frequency rectenna for 2.45- and 5.8-GHz wireless power transmission," *IEEE Trans. Microwave Theory Tech.*, vol. 50, no. 7, pp. 1784–1789, July 2002.

[20] H. Chiou and I. Chen, "High-efficiency dual-band on-chip rectenna for 35- and 94-GHz wireless power transmission in 0.13-μm CMOS technology," *IEEE Trans. Microwave Theory Tech.*, vol. 58, no. 12, pp. 3598–3606, Dec. 2010.

[21] R. Scheeler, S. Korhummel, and Z. Popovic, "A dual-frequency ultralow-power efficient 0.5-g rectenna," *IEEE Microwave Mag.*, vol. 15, pp. 109–114, Jan. 2014.

[22] J. Hagerty, F. Helmbrecht, W. McCalpin, R. Zane, and Z. Popovic, "Recycling ambient microwave energy with broad-band rectenna arrays," *IEEE Trans. Microwave Theory Tech.*, vol. 52, no. 3, pp. 1014–1024, Mar. 2004.

[23] A. Sample and J. Smith, "Experimental results with two wireless power transfer systems," in *Proc. IEEE Radio Wireless Symp.*, Jan. 2009, pp. 16–18.

[24] H. Nishimoto, Y. Kawahara, and T. Asami, "Prototype implementation of ambient RF energy harvesting wireless sensor networks," in *Proc. IEEE Sensors 2010*, pp. 1282–1287.

[25] A. Collado and A. Georgiadis, "Improving wireless power transmission efficiency using chaotic waveforms," in *2012 IEEE MTT-S Int. Microwave Symp. Dig.*, pp. 1–3.

[26] M. S. Trotter, J. D. Griffin, and G. D. Durgin, "Power-optimized waveforms for improving the range and reliability of RFID systems," in *Proc. IEEE Int. Conf. RFID*, Apr. 2009, pp. 80–87.

[27] A. Boaventura, A. Collado, N. Carvalha, and A. Georgiadis, "Optimum behavior," *IEEE Microwave Mag.*, vol. 14, pp. 26–35, Mar. 2013.

[28] H. Matsumoto and K. Takei, "An experimental study of passive UHF RFID system with longer communication range," in *Proc. Asia-Pacific Microwave Conf.*, 2007, pp. 1–4.

[29] T. Ume, H. Yoshida, S. Sikine, Y. Fujita, T. Suzuki, and S. Otaka, "A 950-MHz rectifier circuit for sensor network tags with 10-m distance," *IEEE J. Solid-State Circuits*, vol. 41, no. 1, pp. 35–41, Jan. 2006.

[30] A. Shameli, A. Safarian, A. Rofougaran, M. Rofougaran, and F. De Flaviis, "Power harvester design for passive UHF RFID tag using a voltage boosting technique," *IEEE Trans. Microwave Theory Tech.*, vol. 55, no. 6, pp. 1089–1097, June 2007.

[31] D. Kim, M. A. Ingram, and W. W. Smith Jr., "Efficient far-field radio frequency energy harvesting for passively powered sensor networks," *IEEE J. Solid-State Circuits*, vol. 43, no. 5, pp. 1287–1302, May 2008.

[32] G. Papotto, F. Carrara, and G. Palmisano, "A 90-nm CMOS threshold-compensated RF energy harvester," *IEEE Trans. Solid-State Electron.*, vol. 46, no. 9, pp. 1985–1997, Sept. 2011.

[33] J. Lee, B. Lee, and H. Kang, "A high sensitivity CoSi2-Si Schottky diode voltage multiplier for UHF-band passive RFID tag chips," *IEEE Microwave Wireless Compon. Lett.*, vol. 18, no. 12, pp. 830–832, Dec. 2008.

[34] Y. Yao, J. Wu, Y. Shi, and F. Dai, "A fully integrated 900-MHz passive RFID transponder front end with novel zero-threshold RF-DC rectifier," *IEEE Trans. Ind. Electron.*, vol. 56, no. 7, pp. 2317–2325, July 2009.

[35] H. Nakamoto, D. Yamazaki, T. Yamamoto, H. Kurata, S. Yamada, K. Mukaida, T. Ninomiya, T. Ohkawa, S. Masui, and K. Gotoh, "A passive UHF RF identification CMOS tag IC using ferroelectric RAM in 0.35-μm technology," *IEEE J. Solid-State Circuits*, vol. 42, no. 1, pp. 101–110, Jan. 2007.

[36] U. Karthause and M. Fischer, "Fully integrated passive UHF RFID transponder IC with 16.7-μW minimum RF input power," *IEEE J. Solid-State Circuits*, vol. 38, no. 10, pp. 1602–1608, Oct. 2003.

[37] J. Yi, W. Ki, and C. Tsui, "Analysis and design strategy of UHF micro-power CMOS rectifiers for micro-sensor and RFID applications," *IEEE Trans. Circuits Syst.*, vol. 54, no. 1, pp. 153–166, Jan. 2007.

[38] D. Liu, F. Li, X. Zou, Y. Liu, X. Hui, and X. Tao, "New analysis and design of a RF rectifier for RFID and implantable devices," *Sensors*, vol. 11, pp. 6494–6508, June 2011.

[39] S. Scorcioni, L. Larcher, A. Bertacchini, L. Vincetti, and M. Maini, "An integrated RF energy harvester for UHF wireless powering applications," in *Proc. 2013 IEEE Wireless Power Transfer*, May 2013, pp. 92–95.

[40] H. Lin, K. Chang, and S. Wong, "Novel high positive and negative pumping circuits for low supply voltage," in *Proc. IEEE Int. Symp. Circuits Systems*, 1999, pp. 238–241.

[41] G. Durgin, "The hidden benefits of backscatter radio and RFID at 5.8 GHz," in *Proc. URSI, vol. 48, pp. 1–2,* Jan. 2008.

[42] J. D. Griffin and G. D. Durgin, "Gains for RF tags using multiple antennas," *IEEE Trans. Antennas Propag.*, vol. 56, no. 2, pp. 563–570, Feb. 2008.

[43] J. D. Griffin and G. D. Durgin, "Multipath fading measurements for multi-antenna backscatter RFID at 5.8 GHz," in *Proc. IEEE Int. Conf. RFID*, Apr. 2009, pp. 322–329.

[44] J. D. Griffin, "High-frequency modulated-backscatter communication using multiple antennas," Ph.D. dissertation, Georgia Institute Technol., Georgia, Mar. 2009.

[45] A. Hasan, A. Peterson, and G. Durgin, "Feasibility of passive wireless sensors based on reflected electro-material signatures," *ACES J. Appl. Electromagn.*, vol. 25, no. 6, pp. 552–560, June 2011.

[46] A. Hasan, A. Peterson, and G. Durgin, "Reflected electro-material signatures for self-sensing passive RFID sensors," in *Proc. 2011 IEEE Int. Conf. RFID*, 2011, pp. 62–69.

[47] C. Valenta, P. Graf, M. Trotter, G. Koo, G. Durgin, and B. Schafer, "Backscatter channel measurements at 5.8 GHz across high-voltage corona," in *Proc. IEEE Sensors Conf.*, Nov. 2010, p. 2400.

[48] C. Valenta, P. Graf, M. Trotter, G. Koo, G. Durgin, W. Daly, and B. Schafer, "Transient backscatter channel measurements at 5.8 GHz across high-voltage insulation gaps," in *Proc. AMTA Symp.*, Oct. 2010.

[49] W. Brown and J. Triner, "Experimental thin-film, etched-circuit rectenna," in *1982 IEEE MTT-S Int. Microwave Symp. Dig.*, 1982, pp. 185–187.

[50] T. Ungan, X. Le Polozec, W. Walker, and L. Reindl, "RF energy harvesting design using high Q resonators," in *Proc. IEEE MTT-S Int. Microwave Workshop 2009 Wireless Sensing, Local Positioning, and RFID*, pp. 1–4.

[51] J. Hagerty, "Nonlinear circuits and antennas for microwave energy conversion," Ph.D. dissertation, Univ. Colorado, January 2003.

[52] M. Roberg, T. Reveyrand, I. Ramos, E. Falkenstein, and Z. Povovic, "High-efficiency harmonically terminated diode and transistor rectifiers," *IEEE Trans. Microwave Theory Tech.*, vol. 60, no. 12, pp. 4043–4052, Dec. 2012.

[53] T. Paing, E. Falkenstein, R. Zane, and Z. Popovic, "Custom IC for ultralow-power RF energy scavenging," *IEEE Trans. Power Electron.*, vol. 26, no. 6, pp. 1620–1626, June 2011.

[54] G. Vera, A. Georgiadis, A. Collado, and S. Via, "Design of a 2.45 GHz rectenna for electromagnetic (EM) energy scavenging," in *Proc. IEEE Radio and Wireless Symp.*, 2010, pp. 61–64.

[55] U. Olgun, C. Chen, and J. Volakis, "Wireless power harvesting with planar rectennas for 2.45 GHz RFIDs," in *Proc. 2010 URSI Int. Symp. Electromagnetic Theory*, 2010, pp. 329–331.

[56] U. Olgun, C. Chen, and J. Volakis, "Investigation of rectenna array configurations for enhanced RF power harvesting," *IEEE Antennas Wireless Propag. Lett.*, vol. 10, pp. 262–265, Apr. 2011.

[57] J. Curty, N. Joehl, C. Dehollain, and M. Declercq, "Remotely powered addressable UHF RFID integrated system," *IEEE J. Solid-State Circuits*, vol. 40, no. 11, pp. 2193–2202, Nov. 2005.

[58] S. Mbombolo and C. Park, "An improved detector topology for a rectenna," in *Proc. IMWS-IWPT*, 2011, pp. 23–26.

[59] K. Nishida, Y. Taniguchi, K. Kawakami, Y. Homma, H. Mizutani, M. Miyazaki, H. Ikematsu, and N. Shinohara, "5.8 GHz high sensitivity rectenna array," in *Proc. IMWS-IWPT*, 2011, pp. 19–22.

[60] C. Chin, Q. Xue, and C. Chan, "Design of a 5.8-GHz rectenna incorporating a new patch antenna," *IEEE Antennas Wireless Propag. Lett.*, vol. 4, pp. 175–178, June 2005.

[61] W. Tu, S. Hsu, and K. Chang, "Compact 5.8-GHz rectenna using stepped-impedance dipole antenna," *IEEE Antennas Wireless Propag. Lett.*, vol. 6, pp. 282–284, June 2007.

[62] S. Imai, S. Tamaru, K. Fujimori, M. Sanagi, and S. Nogi, "Efficiency and harmonics generation in microwave to DC conversion circuits of half-wave and full-wave rectifier types," in *Proc. IMWS-IWPT*, 2011, pp. 15–18.

[63] M. Furukawa, Y. Takahashi, T. Fujiware, S. Mihara, T. Saito, Y. Kobayashi, S. Kawasaki, N. Shinohara, Y. Fujino, K. Tanaka, and S. Sasaki, "5.8-GHz planar hybrid rectenna for wireless powered applications," in *Proc. 2006 Asia-Pacific Microwave Conf.*, Dec., pp. 1611–1614.

[64] S. Bharj, R. Camisa, S. Grober, F. Wozniak, and E. Pendleton, "High efficiency C-band 1000 element rectenna array for microwave powered applications," in *IEEE MTT-S Int. Microwave Symp. Dig.*, June 1992, pp. 301–303.

[65] L. Epp, A. Khan, H. Smith, and R. Smith, "A compact dual-polarized 8.51-GHz rectenna for high-voltage (50 V) actuator applications," *IEEE Trans. Microwave Theory Tech.*, vol. 48, no. 1, pp. 111 –120, Jan. 2000.

[66] K. Hatana, N. Shinohara, T. Seki, and M. Kawashima, "Development of MMIC rectenna at 24 GHz," in *Proc. 2013 Radio and Wireless Symp.*, 2013, pp. 199–201.

[67] N. Shinohara, K. Nishikawa, T. Seki, and K. Hiraga, "Development of 24 GHz rectennas for fixed wireless access," in *Proc. 2011 URSI General Assembly Scientific Symp.*, pp. 1–4.

[68] A. Collado and A. Georgiadis, "24 GHz substrate integrated waveguide (SIW) rectenna for energy harvesting and wireless power transmission," in *Proc. 2013 IEEE Int. MTT-S*, pp. 1–3.

[69] Y. Ren, M. Li, and K. Chang, "35 GHz rectifying antenna for wireless power transmission," *Electron. Lett.*, vol. 43, no. 11, pp. 602–603, Nov. 2007.

[70] P. Koert and J. Cha, "Millimeter wave technology for space power beaming," *IEEE Trans. Microwave Theory Tech.*, vol. 40, no. 6, pp. 1251–1258, June 1992.